ISSN 1330-3651 (Print), ISSN 1848-6339 (Online) https://doi.org/10.17559/TV-20210510144005
Original scientific paper

# Effect of Load Distribution Coefficient on Three-Tower Cable-Stayed Bridge with Crossing Cables

Huili WANG*, Wanghua ZHU, Sifeng QIN, Shaobo ZHOU

**Abstract:** The stiffness of the middle tower is lower than the side towers for three-tower cable-stayed bridge. Crossing cables could improve the stiffness of the middle tower. In this paper, the load distribution coefficient of the crossing cables is proposed and its effect on three-tower cable-stayed bridge with crossing cables is investigated. A three-tower cable-stayed bridge with crossing cables is studied with FEM. The geometric nonlinear analysis is carried out with one of the main spans under unbalanced load. Parametric analysis is carried out to present the influence of load distribution coefficient on the deformation of middle tower and main girder. At the same time, the deformation of the middle tower and the main beam of semi-floating system and rigid-frame type is compared. In addition, the effect of reducing the deformation of the middle tower by setting counterweight in the cable crossing zone is also analyzed. The results show that if the load distribution coefficient is 1/2, the displacement of the middle tower under unbalanced load is the minimum. With the increase of the load distribution coefficient, the maximum displacement point of the main girder is close to the mid span. The longitudinal displacement of the middle tower of the semi-floating type is smaller than that of the rigid-frame type. The counterweight in the cross area can reduce the longitudinal displacement of the middle tower.

**Keywords:** crossing cables; deformation; load distribution coefficient; structural stiffness; three-tower cable-stayed bridge

## 1 INTRODUCTION

Three-towercable-stayed bridges have excellent spanning capability with large stiffness. It is an optimal scheme for railway bridge. However, the stiffness of the middle tower is lower than that of the side towers because there is no anchor cable or auxiliary pier for middle tower. The practice has proved that it is an effective approach to install crossing cables at the midspan of each main span [1-4]. At present, the Queensferry Crossing in Scotland is the first three-tower cable-stayed bridge with crossing cables [3, 5, 6]. The Bianyuzhou Changjiang high-speed Railway Bridge under construction in China is a double-tower cable-stayed bridge with crossing cables [7].

The three-tower cable-stayed bridge with crossing cables is a research hotspot of scholars. A preliminary analysis by Gimsing and Georgakis showed that for a three-tower cable-stayed bridge with midspan crossing cables, the longitudinal displacement of the middle tower top will cause redistribution of girder weight among the crossing cables, thus providing constraints for the mid tower [1]. Shaoet al. suggested that the use of crossing cables in some earth-anchored cable-stayed bridges can reduce the axial force on the main girder and increase the total span of double-tower cable-stayed bridges [8]. Chai et al. derived the analytical expression of the longitudinal stiffness constraint of the crossing cables to the bridge tower, which can be used to solve the constraint function of the crossing cables under different tower heights, as well as the analytical solutions of top displacement and mid span deflection of the tower under live load [9, 10]. Cid, C. et al. proposed a method to define the optimal cable system in multi-span cable-stayed bridges, which allows crossed cables in the main spans, different number of cables at each side of the towers and different cable areas [11]. Hiram Arellano et al. proposed that the dead load of the deck at the crossing cables is divided into two parts, which are resisted by each cable anchored at the same anchor point [12].

Up to now, several studies have suggested that it is an effective way to enhance the structure stiffness for three-tower cable-stayed bridge using crossing cables. However, there are limits to how far the influence of load distribution between the crossing cables at the same anchor point can be. The current study aimed to explore the influence of load distribution between crossing cables on the structural stiffness of three-tower cable-stayed bridge. This study made the contributions as follows:

(1) The load distribution coefficient is proposed, and the influence of load distribution between crossing cables on the structural stiffness of three tower cable-stayed bridge is discussed.

(2) The influence of the connection type between beam and tower on the structural stiffness of three tower cable-stayed bridge is compared.

(3) The effect of reducing the deformation of the middle tower by setting counterweight in the cable crossing zone is analyzed.

## 2 DESIGN SCHEME OF THREE-TOWER FOUR-SPAN CABLE-STAYED BRIDGE

The conceptual design scheme of a three tower four span cable-stayed bridge is shown in Fig. 1. The total length of the bridge is 1342 m, and the span arrangement is 35 m + 177 m + 459 m + 459 m + 177 m + 35 m. At the tower position, the semi-floating type is adopted, which only vertical support sets on the tower for the main girder. The tower is a reinforced concrete structure with a height of 170.3 m, 125.8 m above the bridge deck. The cables are arranged in fan-shaped double cable planes, totalling 216 ($18 \times 2 \times 6$). Four pairs of crossing cables are set at the midspan, and the width of the cable crossing zone is 105 m. The main girder is a steel box girder, 4.5 m high and 39 m wide, as shown in Fig. 2. The parameters of the section and materials are shown in Tab. 1. A plane Cartesian coordinate system is set, whose origin is the root of the middle tower.

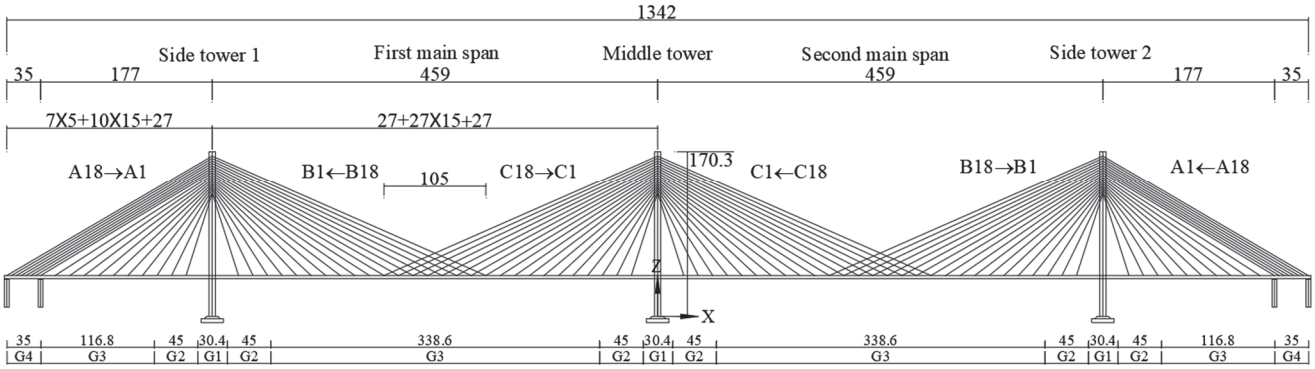


**Figure 1** Schematic diagram of elevation layout of three-tower four-span cable-stayed bridge / m

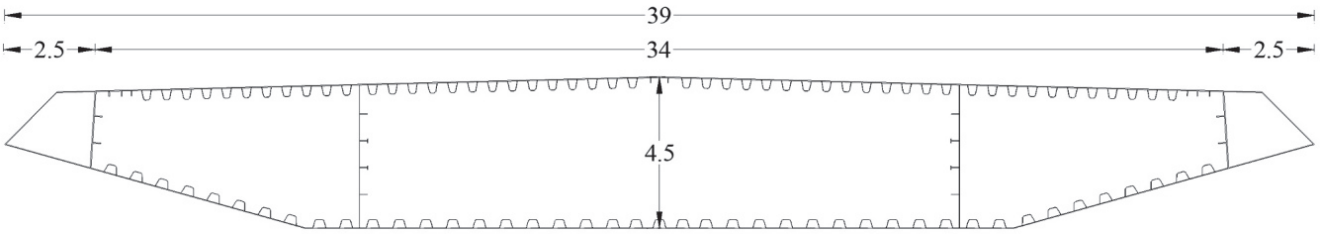


**Figure 2** General section of main beam / m

**Table 1** Section and material parameter table

| Section | Material | Elastic modulus / GPa | Poisson's ratio | Area / m$^2$ | $I_{yy}$ / m$^4$ | $I_{zz}$ / m$^4$ | $I_{xx}$ / m$^4$ |
|---|---|---|---|---|---|---|---|
| G1 | Steel (Q345) | 206 | 0.3 | 2.328 | 8.095 | 252.005 | 24.386 |
| G2 | | | | 1.966 | 6.661 | 217.406 | 20.129 |
| G3 | | | | 1.911 | 6.356 | 214.762 | 19.371 |
| G4 | | | | 2.204 | 7.874 | 220.83 | 22.678 |
| Upper cross beam | | | | 0.761 | 2.055 | 1.79764 | 2.502 |
| Tower top | Concrete (C50) | 34.5 | 0.2 | 15.210 | 80.344 | 41.8089 | 101.992 |
| Tower base | | | | 29.650 | 285.205 | 147.606 | 347.080 |
| Lower cross beam | | | | 20.309 | 85.987 | 96.565 | 156.602 |
| Stay cable | Steel wire (Strand1860) | 195 | 0.3 | 0.012 | - | - | - |

Note: The yield stress of Strand1860 is 1860 MPa. The yield stress of Q345 is 345 MPa. The design compressive strength of C50 is 22.4 MPa. $I_{yy}$, $I_{zz}$ and $I_{xx}$ denote the moment of inertia. G1-G4 is beam section number. A1-A18, B1-B18, C1-C18 is the cable number.

## 3 MECHANISM OF CROSSING CABLES

Let's assume the cable force increment is $\Delta T_{L_i}$ in the cable $L_i$. For traditional cable-stayed bridge, the vertical force at point $i$ is $P = \Delta T_{L_i} \sin\alpha$, as shown in Fig. 3a.

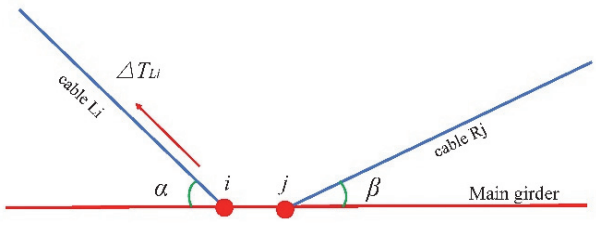


(a) Traditional cable-stayed bridge

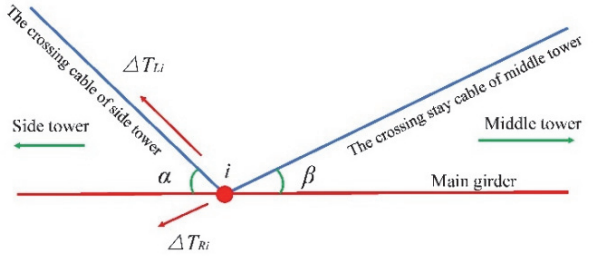


(b) Cable-stayed bridge with crossing cables

**Figure 3** Mechanism of crossing cables

However, for cable-stayed bridge with crossing cables, if the cable force increment is $\Delta T_{L_i}$ in the cable $L_i$, the cable force decrement is $\Delta T_{R_i}$ in the cable $R_i$ due to internal forces redistribution caused by the deformation of mid-tower, as shown in Fig. 3b, [13]. Thus, the vertical force at point $i$ is $P' = \Delta T_{L_i} \sin\alpha - \Delta T_{R_i} \sin\beta$. Obviously, $P > P'$, so the deformation of traditional cable-stayed bridge is larger than cable-stayed bridge with crossing cables. That means the crossing cables enhance the stiffness of cable-stayed bridge.

## 4 DEFINITION OF LOAD DISTRIBUTION COEFFICIENT

At the cable crossing zone, the dead load of the main girder is divided into two parts. Such loads are resisted by each cable anchored at the same point. According to the simplified mechanical model shown in Fig. 4, Eq. (1) can be easily derived from the vertical force balance under the premise of ignoring the bending resistance of the main girder.

$$T_{L_i} \cdot \sin\alpha + T_{R_i} \cdot \sin\beta = G_i \tag{1}$$

where $T_{L_i}$ is the crossing stay cable force of the side tower, $T_{R_i}$ is the crossing stay cable force of the middle tower, $G_i$ is the dead load of the beam section at node $i$, and $\alpha$ and $\beta$ are the angle between the stay cable and the main girder.

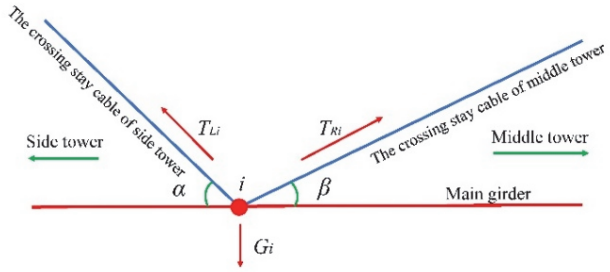


**Figure 4** Load distribution in crossing cables

There is axial force on the main girder, so the longitudinal component of the crossing stay cable force may not be equal. If $T_{L_i}\cos\alpha \neq T_{R_i}\cos\beta$, the cable force cannot be solved. The load distribution coefficient is represented by $\eta$, which is the ratio of the dead load shared by the crossing cables. The cable forces of crossing cables anchored at the same point are obtained according to Eq. (2) and Eq. (3).

$$T_{L_i}\sin\alpha = \eta G_i \Rightarrow T_{L_i}(\eta) = \frac{\eta G_i}{\sin\alpha} \tag{2}$$

$$T_{R_i}\sin\beta = (1-\eta)G_i \Rightarrow T_{R_i}(\eta) = \frac{(1-\eta)G_i}{\sin\beta} \tag{3}$$

Note: $0 < \eta < 1$

## 5 EFFECT OF LOAD DISTRIBUTION COEFFICIENT ON THE STIFFNESS OF CABLE-STAYED BRIDGES

In order to study the effect of load distribution coefficient on the stiffness of cable-stayed bridges, a finite element model is established according to the five load distribution coefficients: 1/6, 2/6, 3/6, 4/6 and 5/6. The reasonable completed bridge state is obtained by using the influence matrix method [14, 15]. If one of the main spans is under load, the maximum deformation of the three-tower cable-stayed bridge would occur. In this paper, a uniform load is applied to the second main span, and the load concentration is taken as 50 kN/m, [9]. The deformation diagram of the structure under load is shown in Fig. 5.

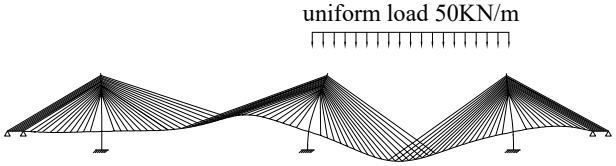


**Figure 5** Schematic diagram of bridge structure deformation under unbalanced load

In performing geometric nonlinear analysis of the finite element model under live load, the following factors are considered: (1) The sag effect of cables; (2) The $P-\Delta$ effect of main beam or tower under the action of huge axial pressure; (3) The large displacement effect of structure.

In this paper, the rigid-frame type is also analyzed, the tower of which is completely consolidated with the main girder.

## 6 DEFORMATION RESULTS OF THE MIDDLE TOWER

The longitudinal displacement of the middle tower varies with load distribution coefficient, and the results are plotted in Fig. 6. The results show that if the load distribution coefficient is 3/6, the displacement of the middle tower is the minimum. With the increase of the load distribution coefficient, the longitudinal displacement of the middle tower first decreases and then increases, and the difference between the maximum value and the minimum value is nearly 10 cm. In addition, by comparing the calculation results of the two types of the middle tower, it is found that the tower top displacement of the semi-floating type is about 20% less than that of the rigid-frame type.

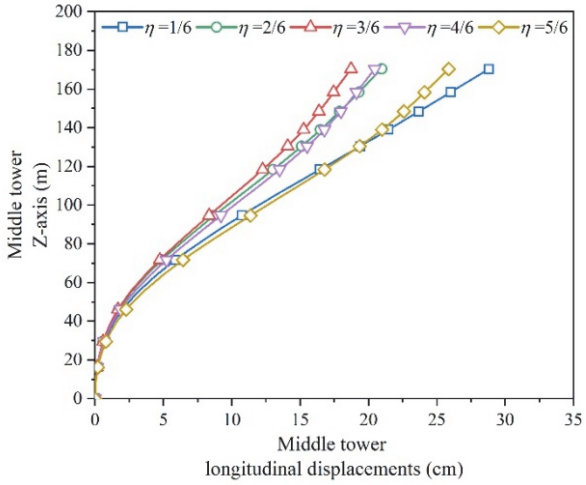


(a) Semi-floating type

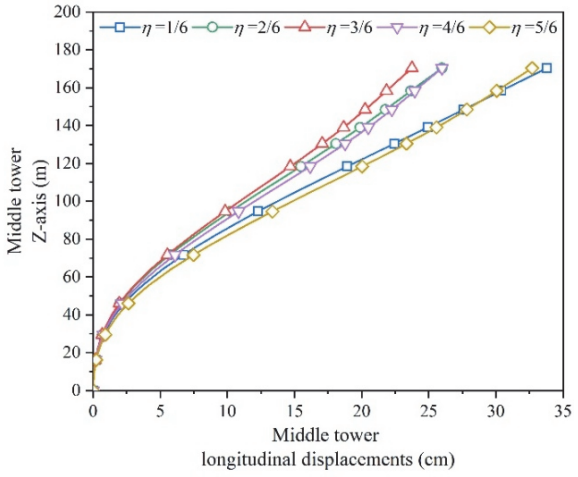


(b) Rigid-frame type

**Figure 6** Longitudinal displacements of middle tower

To further study the effect of the load distribution coefficient on the longitudinal displacement of the middle tower, Fig. 7 shows the calculation results of tower top displacement from three types of analysis. The results of the three analysis types include: (1) The results of geometric linear analysis; (2) The results of considering sag effect on the basis of geometric linear analysis; (3) The results of geometric nonlinear analysis.

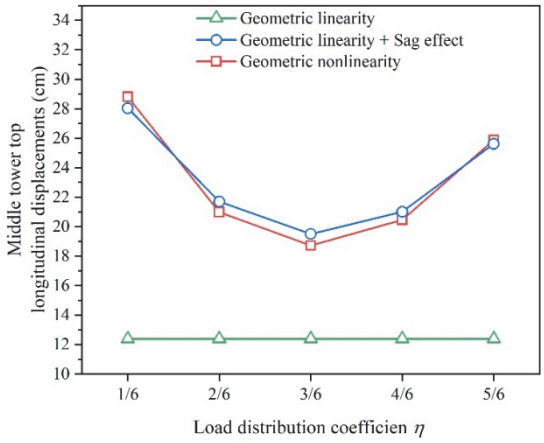


(a) Semi-floating type

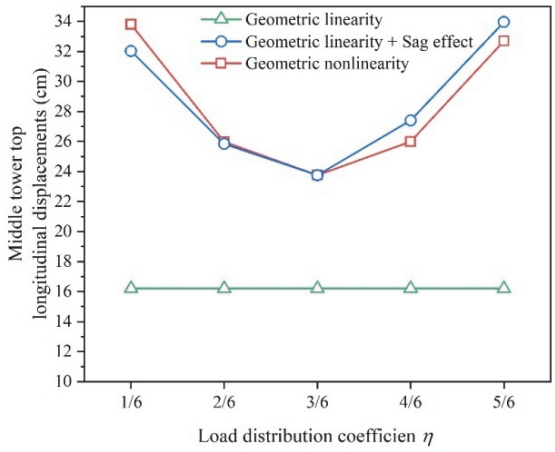


(b) Rigid-frame type

**Figure 7** Longitudinal displacements of middle tower top

It can be seen from Fig. 7 that the results of geometric linear analysis with sag effect are close to those of geometric nonlinear results, while the results of geometric linear analysis are not affected by the load distribution coefficient. So cable sag effect is the main factor which leads to the change of tower displacement with load distribution coefficient. This is because the cable sag affects the axial stiffness of the stay cable, which varies with the load distribution coefficient. Chai also pointed that the axial stiffness of the cross cable affects the structural stiffness of the middle tower [9, 10].

## 7 DEFORMATION RESULTS OF THE MAIN GIRDER

According to the finite element calculation results, the vertical displacement of the main girder is extracted. Fig. 8 and Fig. 9 show the vertical displacement occurs at the two main spans if the load is applied to the second main span. The position of the maximum displacement of the two main spans on the *X* axis has been marked with a dotted line in the figure. Tab. 2 lists the coordinates and the maximum displacement value of the maximum displacement position on the *X* axis.

It can be seen from Fig. 8, Fig. 9 and Tab. 2 that with the increase of load distribution coefficient, the maximum vertical displacement of the first main span decreases first and then increases. On the contrary, the maximum vertical displacement of the second main span under load increases first and then decreases.

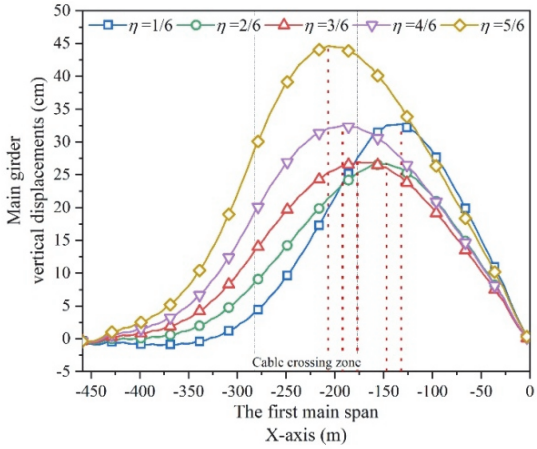


(a) Semi-floating type

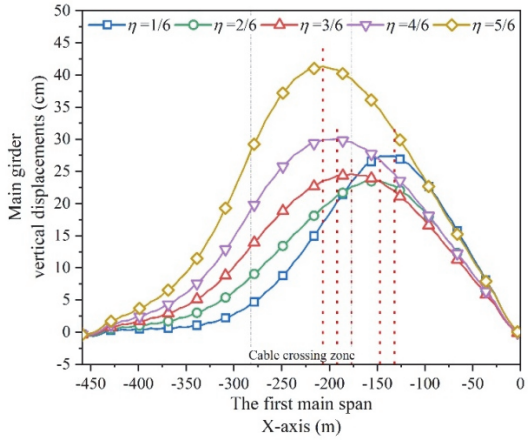


(b) Rigid-frame type

**Figure 8** Vertical displacements of the first main span

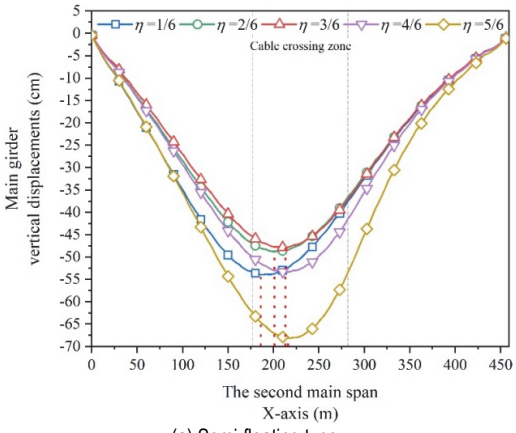


(a) Semi-floating type

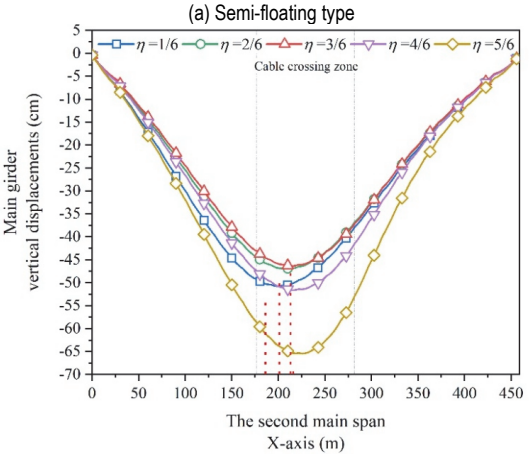


(b) Rigid-frame type

**Figure 9** Vertical displacements of the second main span

**Table 2** Displacement comparison

| Position | Structural type | Item | Unit | Load distribution coefficient $\eta$ | | | | |
|---|---|---|---|---|---|---|---|---|
| | | | | 1/6 | 2/6 | 3/6 | 4/6 | 5/6 |
| First main span | Semi-floating type | Maximum value | cm | 32.7 | 26.7 | 26.9 | 32.5 | 44.6 |
| | | *X*-axis coordinate | m | –132 | –147 | –177 | –192 | –207 |
| | Rigid-frame type | Maximum value | cm | 27.4 | 23.6 | 24.6 | 30.1 | 41.3 |
| | | *X*-axis coordinate | m | –132 | –147 | –177 | –192 | –207 |
| Second main span | Semi-floating type | Maximum value | cm | –53.9 | –48.8 | –47.9 | –53.4 | –68.2 |
| | | *X*-axis coordinate | m | 186 | 201 | 213 | 213 | 216 |
| | Rigid-frame type | Maximum value | cm | –50.7 | –47.0 | –46.4 | –51.6 | –65.5 |
| | | *X*-axis coordinate | m | 201 | 213 | 213 | 216 | 226 |

In addition, with the increase of the load distribution coefficient, the stiffness of the crossing cables of the middle tower increases. Thus, the stiffness of the main girder near the middle tower increases, and the maximum displacement point is gradually away from the middle tower and is close to the center of the main span.

Comparing the calculation results of the two structural types, it can be seen that the displacement of the main girder using the semi-floating type is larger than that of the rigid-frame type. This shows that the semi-floating type can reduce the longitudinal displacement of the middle tower top by about 15% - 21%; however it will increase the vertical displacement of main girder by 8% - 19%.

## 8 INFLUENCE OF COUNTERWEIGHT IN CABLE CROSSING ZONE ON DISPLACEMENT OF MIDDLE TOWER

Because the two cables in the cable crossing zone are anchored at the same anchor point, the force of the crossing cables is less than that of the nearby non-crossing cables. At the same time, the crossing cables are the longest cables in the bridge, and the sag effect of the cables is significant. In order to increase the axial stiffness of the crossing cables, the uniformly distributed load $q$ is used as the counterweight at the intersection area of the two main spans. The load acts on the second main span, and the displacement results of the middle tower top are shown in Fig. 10. Only the calculation results of load distribution coefficient of 3/6 are given in the figure.

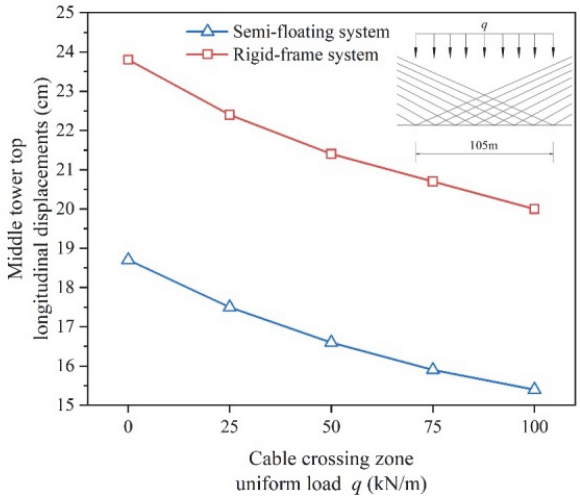


**Figure 10** Longitudinal displacement of the top of the middle tower under different uniform load

It can be seen from Fig. 10 that the longitudinal displacement of the middle tower can be reduced by setting counterweight in the cable crossing zone. If the uniform load q increases from 0 kN/m to 100 kN/m, the longitudinal displacement of the middle tower decreases by 16%.

## 9 CONCLUSION

(1) With the increase of load distribution coefficient, the longitudinal displacement of the middle tower first decreases and then increases. If the load distribution coefficient is 3/6, the displacement of the middle tower under unbalanced load is the minimum.

(2) With the increase of the load distribution coefficient, the crossing stay cable force increases, the structural stiffness of the main girder near the middle tower increases, and the maximum displacement point of the main girder is close to the mid span.

(3) The tower top displacement of the semi-floating type is about 20% less than that of the rigid-frame type.

(4) The counterweight in the cross area can increase the stiffness of the crossing stay cable, which can reduce the longitudinal displacement of the middle tower.

## Acknowledgements

This work is supported by the Liaoning Provincial Doctoral Scientific Foundation Projects (20170520138) and the Liaoning Provincial Natural Science Foundation Guidance Projects (2019-ZD-0006).

## 10 REFERENCES

[1] Gimsing, N. J. & Georgakis, C. T. (2011). *Cable Supported Bridges: Concept and Design, Third Edition*. Cable Supported Bridges: Concept and Design, Third Edition. John Wiley and Sons. https://doi.org/10.1002/9781119978237

[2] Virlogeux, M. (2001). Bridges with multiple cable-stayed spans. *Structural Engineering International: Journal of the International Association for Bridge and Structural Engineering (IABSE)*, *11*(1),61-82. https://doi.org/10.2749/101686601780324250

[3] Carter, M., Kite, S., Hussain, N., & Minto, B. (2010). Design of the Forth replacement crossing, Scotland. *Proceedings of the Institution of Civil Engineers: Bridge Engineering*, *163*(2), 91-99. https://doi.org/10.1680/bren.2010.163.2.91

[4] Shao, X., Deng, F., & Deng, L. (2018). Conceptual Design of a New Three-Tower Cable-Stayed Bridge System with Unequal-Size Fans. *Journal of Bridge Engineering*, *23*(7). https://doi.org/10.1061/(ASCE)BE.1943-5592.0001257

[5] Kite, S., Hussain, N., & Carter, M. (2011). Forth Replacement Crossing - Scotland, UK. *12th East Asia-Pacific Conference on Structural Engineering and Construction, EASEC12*, 1480-1484. https://doi.org/10.1016/j.proeng.2011.07.186

[6] Kite, S., Carter, M., & Hussain, N. (2010). Design of the forth replacement crossing, Scotland, UK. *34th International Symposium on Bridge and Structural Engineering: Large*

*Structures and Infrastructures for Environmentally Constrained and Urbanised Areas*, 202-203. https://doi.org/10.2749/101686610791283551
[7] Ning, B.-W. (2020). Overall Design of Bianyuzhou Changjiang River Bridge on Newly-Built Anqing-Jiujiang High-Speed Railway. *Bridge Construction*, *50*(1), 86-91.
[8] Shao, X., Hu, J., Deng, L., & Cao, J. (2014). Conceptual design of superspan partial ground-anchored cable-stayed bridge with crossing stay cables. *Journal of Bridge Engineering*, *19*(3). https://doi.org/10.1061/(ASCE)BE.1943-5592.0000534
[9] Chai, S. & Wang, X. (2019). Simplified calculation method for deformation of multi-tower cable-stayed bridges with crossed cables. *Engineering Structures*, 181, 354-361. https://doi.org/10.1016/j.engstruct.2018.12.030
[10] Chai, S., Xiao, R., & Wang, X. (2016). Longitudinal restraint stiffness of crossed cables in multi-tower cable-stayed bridge. *Harbin Gongye Daxue Xuebao/Journal of Harbin Institute of Technology*, *48*(9), 119-124. https://doi.org/10.11918/j.issn.0367-6234.2016.09.021
[11] Cid, C., Baldomir, A., & Hernandez, S. (2018). Optimum crossing cable system in multi-span cable-stayed bridges. *Engineering Structures*, *160*, 342-355. https://doi.org/10.1016/j.engstruct.2018.01.019
[12] Arellano, H., Tolentino, D., & Gomez, R. (2019). Optimum Criss Crossing Cables in Multi-span Cable-stayed Bridges using Genetic Algorithms. *KSCE Journal of Civil Engineering*, *23*(2), 719-728. https://doi.org/10.1007/s12205-018-5736-2
[13] Hengda, C., Sisi, Y., & Xiaoguang, W. (2018). The stress mechanism and parameter analysis of multi-tower cable-stayed bridge with crossed cables. *Journal of Railway Science and Engineering*, *15*(10). https://doi.org/10.19713/j.cnki.43-1423/u.2018.10.014
[14] Yang, J. (2010). Determining the rational completion cable forces based on influence matrix method united minimum bending energy method. *Traffic and Transportation Studies 2010 - Proceedings of the 7th International Conference on Traffic and Transportation Studies*, 1417-1424. https://doi.org/10.1061/41123(383)136
[15] Wang, H.-L. & Qin, S.-F. (2016). Shape finding of suspension bridges with interacting matrix. *European Journal of Environmental and Civil Engineering*, *20*(8), 831-840. https://doi.org/10.1080/19648189.2015.1084379

**Contact information:**

**Huili WANG**
(Corresponding author)
National & Local Joint Engineering Laboratory of Bridge and Tunnel Technology, State Key Laboratory of Structural Analysis for Industrial Equipment, Dalian University of Technology, Dalian, China
E-mail: wanghuili@dlut.edu.cn

**Wanghua ZHU**
National & Local Joint Engineering Laboratory of Bridge and Tunnel Technology, Dalian University of Technology, Dalian, China
Beijing General Municipal Engineering Design & Research Institute Co., Ltd, Beijing, China

**Sifeng QIN**
College of Civil Engineering and Architecture,
Dalian University, Dalian, China

**Shaobo ZHOU**
National & Local Joint Engineering Laboratory of Bridge and Tunnel Technology, Dalian University of Technology, Dalian, China